Electronic Supplementary Information

Biosensor surface functionalization by a simple photochemical immobilization of antibodies: An Experimental characterization by Mass Spectrometry and Surface Enhanced Raman Spectroscopy

B. Della Ventura,[1] M. Banchelli,[2] R. Funari,[3]† A. Illiano,[4] M. De Angelis,[2] P. Taroni,[1] A. Amoresano,[4] P. Matteini,[2] R. Velotta[3]

[1]Dipartimento di Fisica, Politecnico di Milano, Piazza Leonardo da Vinci 32, 20133 – Milano (Italy)

[2]IFAC-CNR, Istituto di Fisica Applicata 'Nello Carrara', via Madonna del Piano 10 , 50019, Sesto Fiorentino, (Italy)

[3]Dipartimento di Fisica "Ettore Pancini" – Via Cintia, 26 Ed. 6 - 80126 – Napoli (Italy) Italy

[4]Dipartimento di Scienze Chimiche – Via Cintia, 26 Ed. 6 - 80126 – Napoli (Italy) Italy

*Corresponding author: rvelotta@unina.it

†Present Address: Okinawa Institute of Science and Technology, Graduate University, 1919-1 Tancha, Onna-son, Okinawa, 904-0495 Japan.

Contents

Advantages of MALDI-TOF-MS for Ab mapping

By using last generation LC-ES-TOF mass spectrometers, the mass of intact antibodies can be measured with a precision reaching 40 ppm, which speeds-up considerably the screening and routine monoclonal antibodies identification. Peptide mass fingerprinting (PMF) performed by using liquid chromatography–mass spectrometry (LC-MS) is nowadays the standard analytical method for protein mapping. PMF is generally performed by comparing mass values detected in the chromatograms of peptides after enzymatic digestion with theoretical values. However, this method suffers from some limitations, namely it is time-consuming and laborious due to long gradient time needed for HPLC separation and the extensive search to find a characteristic mass shift.[1] Thus, alternative strategies have been exploited. In this context, MALDI-TOF MS analyses combined with reflectron tools is a widely adopted technology used in proteomics.[2–4] This technique provides promising qualitative results resulting in the preferred solution for protein mapping because it offers a unique speed advantage over LC-MS in terms of greatly reduced instrument time and high accuracy and resolution. MALDI-TOF mass measurements are less accurate when applied to the intact antibody (2 heavy and 2 light chain), but provides direct information on the light chain mass and fragments. After disulfide bridge reduction, very acute data can be recorded for both light (25 kDa range) and heavy chains (50 kDa range). In addition, the efficacy of mass spectrometry over classical electrophoresis and liquid-chromatography methods has also recently demonstrated for posttranslational modifications that were not previously reported for monoclonal antibodies.

Constant region heavy chain (IGH1M):

AKTTPPSVYP LAPGSAAQTN SMVTLGCLVK GYFPEPVTVT WNSGSLSSGV HTFPAVLQSD LYTLSSSVTV PSSPRPSETV TCNVAHPASS TKVDKKIVPR DCGCKPCICT VPEVSSVFIF
PPKPKDVLTI TLTPKVTCVV VDISKDDPEV QFSWFVDDVE VHTAQTQPRE EQFNSTFRSV SELPIMHQDW LNGKEFKCRV NSAAFPAPIE KTISKTKGRP KAPQVYTIPP PKEQMAKDKV
SLTCMITDFF PEDITVEWQW NGQPAENYKN TQPIMNTNGS YFVYSKLNVQ KSNWEAGNTF TCSVLHEGLH NHHTEKSLSH SPGLQLDETC AEAQDGELDG LWTTITIFIS LFLLSVCYSA
AVTLFKVKWI FSSVVELKQT LVPEYKNMIG QAP

Constant region light chain (IGKC):

ADAAPTVSIF PPSSEQLTSG GASVVCFLNN FYPKDINVKW KIDGSERQNG VLNSWTDQDS KDSTYSMSST LTLTKDEYER HNSYTCEATH KTSTSPIVKS FNRNEC

Variable region heavy chain (HVAR):

VKLQESGAEL ARPGASVKMS CKASGYTFTT YTIHWIKQRP GQGLEWIGYI NPSSVYTNYN QRFKDKATLT RDRSSNTANI HLSSLTSDDS AVYYCVREGE VPYWGQGTTV TVSSAKTTPP

Variable region light chain (LVAR):

KCAHTVSKSM SMSVGERVTL TCKASENVVT YVSWYQQKPE QSPKLLIYGA SNRYTGVPDR FTGSGSATDF TLTISSVQAE DLADYHCGQG YSYPYTFGGG TKLEIKRADA

FIG S1. Sequence of monoclonal antibody anti-phenobarbital from host musculus. Database code: 1IgY. The cysteines and the tryptophan forming triads are highlighted in yellow and green, respectively.

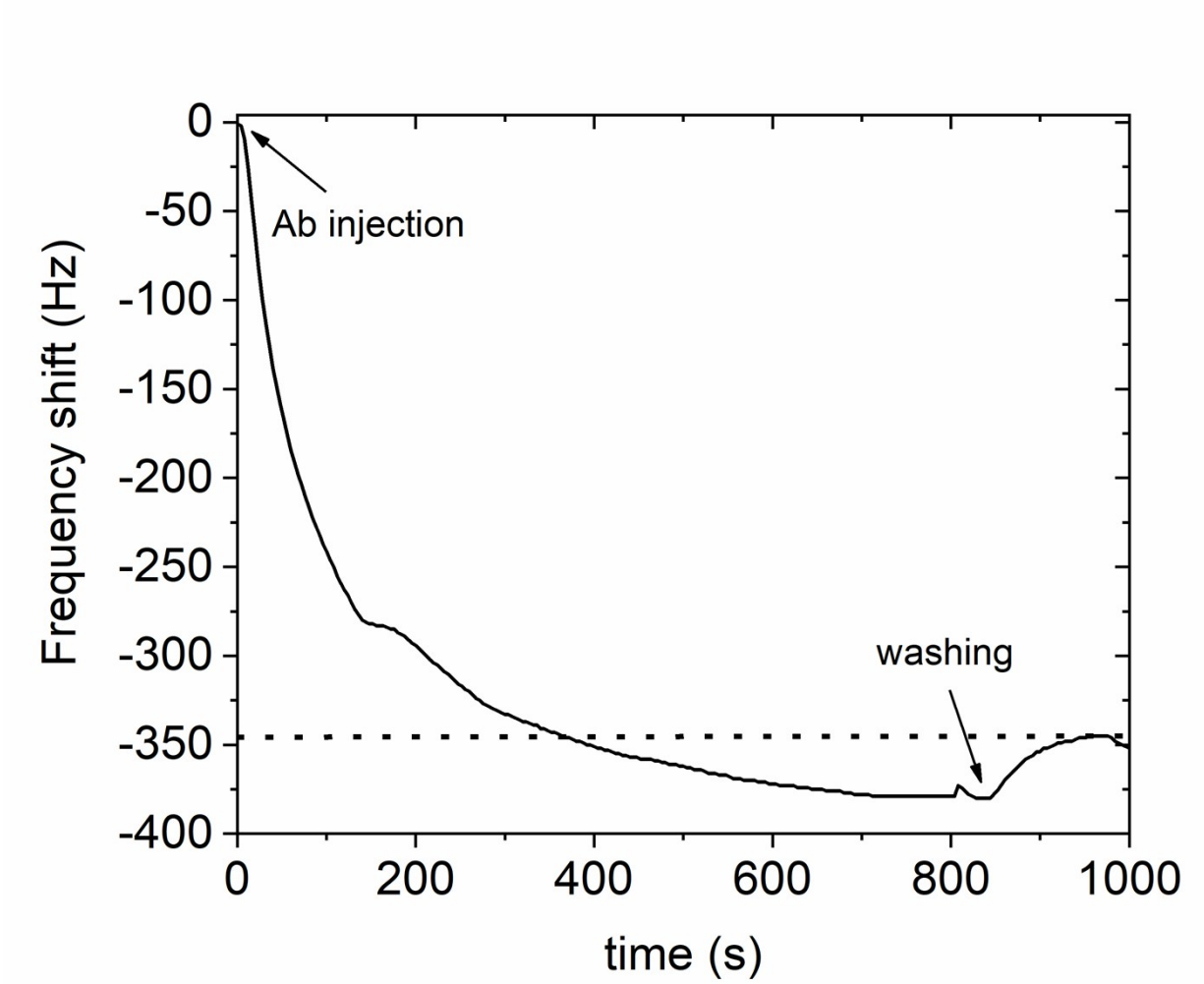

FIG S2. Sensorgram recorded during the surface functionalization of a AgNCs-decorated QCM substrate. After the stabilization of the oscillation frequency in milli-Q water, the Ab solution (25 μg/mL) irradiated by UV lamp for 30 s was promptly injected in the cell causing an immediate frequency drop, the latter measuring the Ab-surface binding. From the Ellman's assay it turns out that the thiol groups are still reactive within a 300 s, a time long enough to almost approach the equilibrium value of approximately -350 Hz. The equilibrium value is evaluated after the washing step that removes possible weakly tethered IgGs. In agreement with our previous experiments, similar sensorgram was also recorded with untreated Abs, which tether the surface by simple physisorption.[5–7]

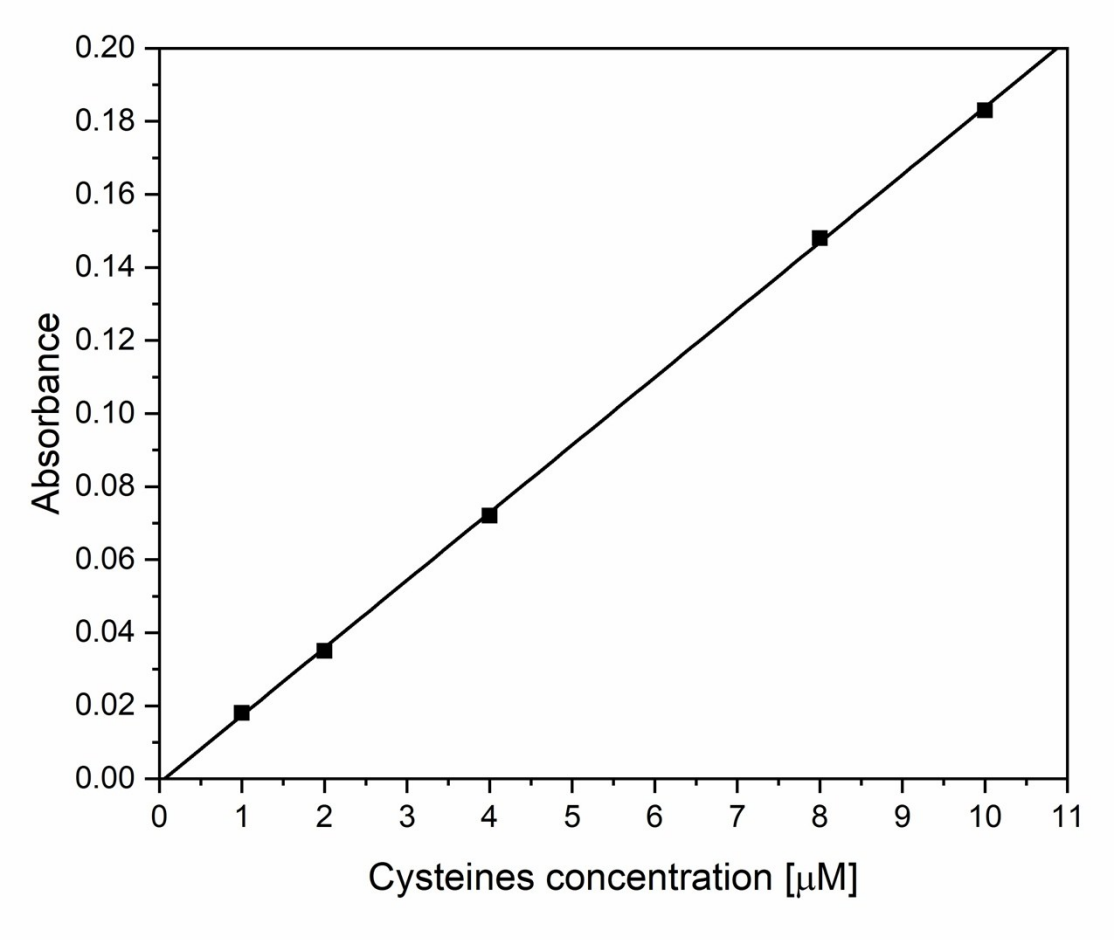

FIG S3. Calibration curve for the Ellman's assay. Absorption at 412 nm of anion TNB^{2-} resulting from reaction of free cysteines with DTNB for 15 minutes. The error bars are within the thickness of the data points.

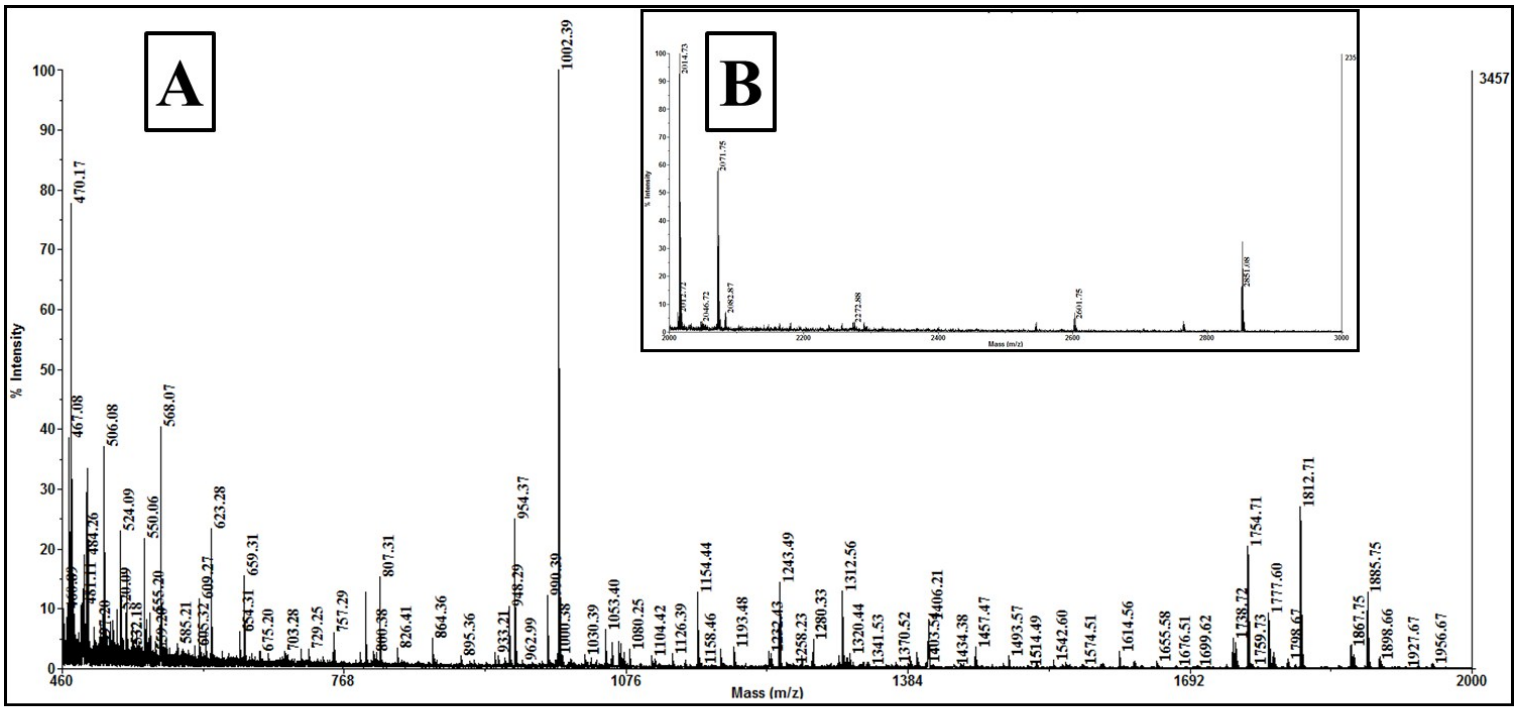

C

IGKC	m/z	%INTENSITY	PEPTIDE
30 s 30 µg	568.07	100	
	926.30	6	[100-106] C*106
	1312.56	5	[81-91]C86
	1370.52	<5	[81-91]C*86
	1405.59	<5	[1-28]C*26
IGH1M	**m/z**	**% INTENSITY**	**PEPTIDE**
30 s 30 µg	568.07	100	
	550.06	37	[355-358]- C*357
	1070.43	<5	[355-364] C*357
	1037.42	<5	[301-309]C*302
	1405.59	<5	[101-125]C*102-107
	1885.77	5	[12-30]C27/[325-341]C*330
	2071.77	<5	[325-342]C*330
	2851.10	<5	[62-92]C82

FIG S4. MALDI-TOF mass spectrometry spectrum of 25 ug/mL of IgG standard proteins digested with trypsin and chymotrypsin and exposed to UV radiation for 30 s. Panel A shows the entire explored mass range [450-3000]m/z. Panel B is a mass spectrum enlargement in [2100-3000] m/z region. Panel C shows mass attribution related to the peaks containing cysteine.

Synthesis and characterization of AgNCs

Ethylene glycol was purchased by Schaefer while all the other reagents were purchased by Sigma-Aldrich and used without any further purification. Synthesis of silver nanocubes was performed by following a published procedure.[8,9] Briefly, ethylene glycol (10ml) was placed into a flask and heated under magnetic stirring in an oil bath at 150°C for 1 hour, in a nitrogen flow. Sodium sulfide (0.175 ml of 0.72 mg/ml solution) and polyvinylpyrrolidone (PVP 55000 MW, 3.75 ml of 20 mg/ml solution) were subsequently added to the flask. A freshly prepared silver nitrate solution was added dropwise into the reaction flask (1.25 ml of a 48 mg/ml solution). The reaction was stopped after 40 min in an ice-bath by adding 30 ml of acetone. Nanoparticles were centrifuged at 10000 g for 30 min and dispersed in ethanol using an ultrasonic bath. The washing procedure was repeated three times to remove all the reagents and the obtained yield of the reaction was around 80% for the silver nanocubes. The suspension of silver nanocubes was stored at -18°C. Size and shape of the as-prepared nanoparticles were analyzed by transmission electron microscopy. The optical properties of the nanoparticles were characterized by a Jasco V-560 spectrophotometer.

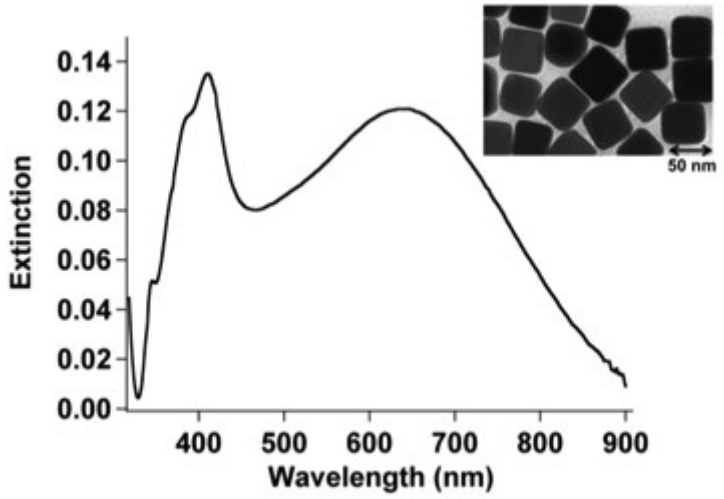

FIG S5. Extinction spectrum of a dispersion of AgNCs once deposited onto a quartz slide and TEM image of the as-synthesized particles (inset).

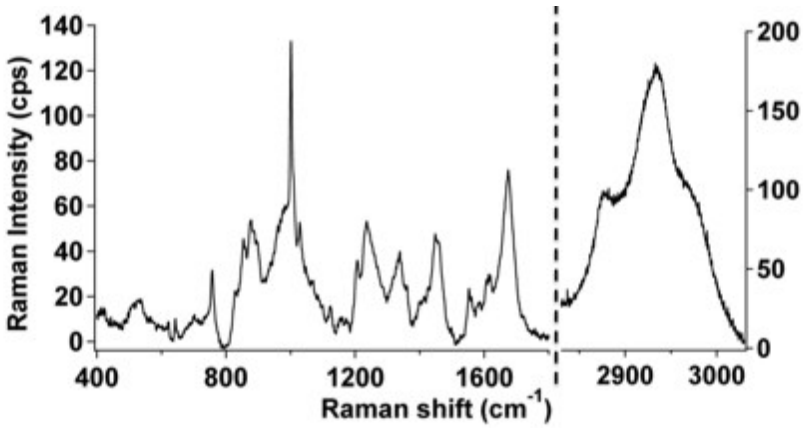

FIG S6. Raman spectrum (λ_{EX} = 532 nm) of a dried deposit of monoclonal IgG on a gold mirror support.

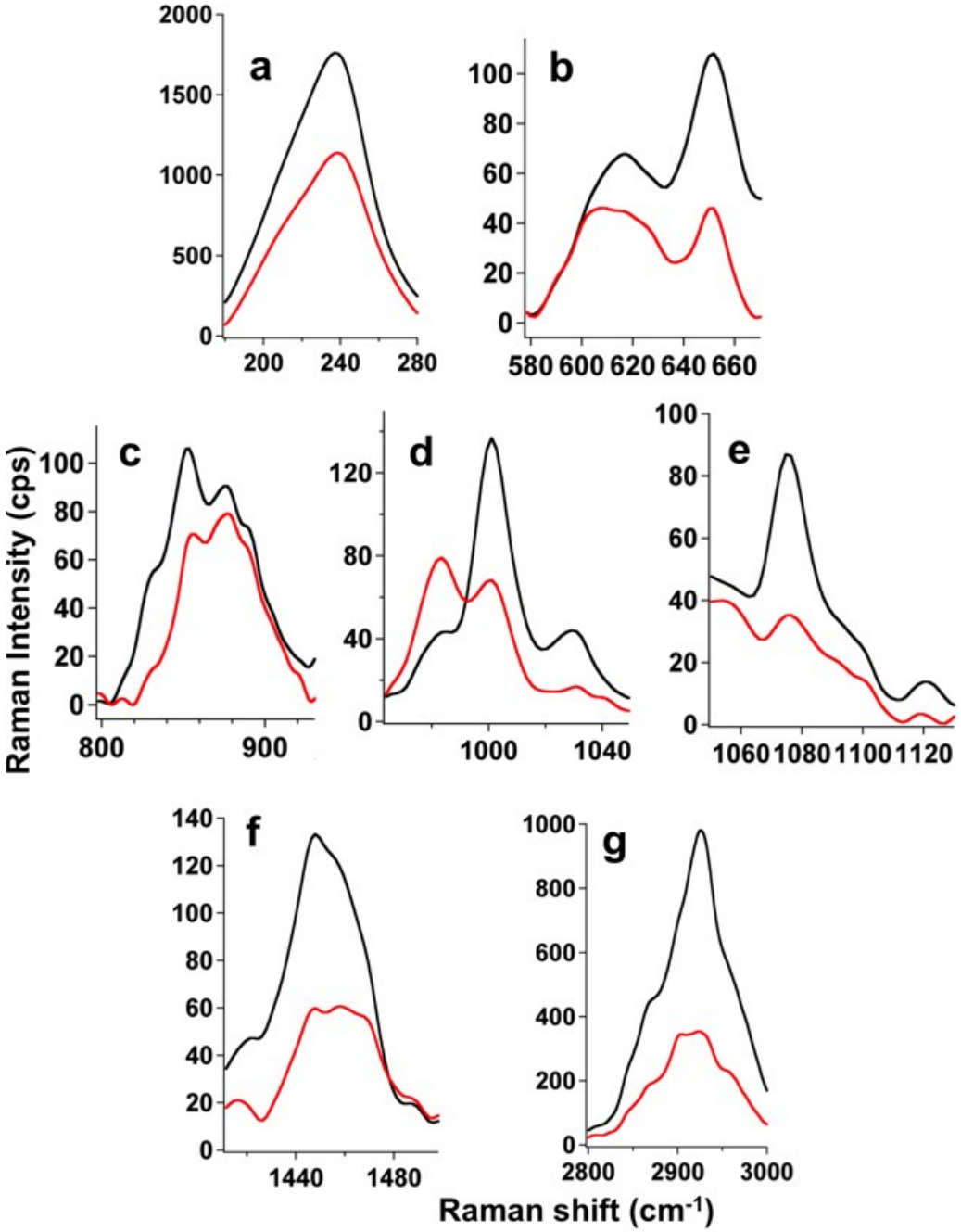

FIG S7. SERS profiles of UV-treated (black, , labelled as "UV") and untreated (gray) IgG over different vibrational spectral ranges (λ_{EX} = 532 nm; integration time = 10 s; laser power at the sample ≈ 2 mW).

Assignment	Raman (cm^{-1})	SERS (cm^{-1})
ν(AgX), X=N,O,S	/	220-260
ν(SS)	531	/
ν(CS)	642	653
W	756	756
Y	829,853	829,853
W	877	877
Amide III β-sheet	/	985
F	1003,1031	1003,1031
ν(CN) (N,R,K,H)	1121	1079,1129
Y	/	1173
F,Y	1205	1205
Amide III β-sheet	1235	1237
Amide III α-helix, random	/	1271
Amide III β-sheet, turn	/	1302
β(CH), W	1337	1330
α,β (CH_2/CH_3)	1447	1447
W	1552	1555
F,Y	1612	1602
Amide I α-helix, random		1650
Amide I β-sheet, turn	1674	1674
ν(CH_2/CH_3)	2820-2980	2820-2980

Table S1. Vibrational mode assignment of Raman and SERS (λ_{EX} = 532 nm) signals of IgG.[10–15]

	Vibrational mode	Integration range (cm^{-1})	UV-treated / untreated IgG
a	ν(Ag-S)	180-300	1.5±0.1
b	ν(C-S)	620-680	1.6±0.1
c	Y	830-850	1.5±0.1
d	F	1003-1031	3.0±0.1
e	ν(C-N)	1050-1100	3.1±0.1
f	def(C-H)	1410-1470	2.4±0.1
g	ν(C-H)	2800-3000	2.7±0.1

Table S2. Ratio between the SERS integrated signals (λ_{EX} = 532 nm) of UV-treated and untreated IgG sample within different spectral ranges (listed according to Fig. S5). The values were calculated by considering the integrated areas of deconvoluted bands ascribed to the vibrational modes as listed in the 2nd column.

	Assignment	Frequency (cm^{-1})	control IgG (%)	UV-activated IgG (%)
Amide I	α-helix/random	1650	15	17
	β-sheet	1674	85	83

Table S3. Analysis of the SERS signals (λ_{EX} = 532 nm) of UV-activated and control IgG samples in the Amide I region. Percentage of secondary structures are calculated by multipeak fitting analysis through band deconvolution by Lorentzian functions.

References

1 L. Dai, R. Preston, M. Bacica, A. Kinhikar, B. Bolaños and R. E. Murphy, *Bioconjug. Chem.*, 2013, **24**, 53–62.

2 W. Pusch and M. Kostrzewa, *Curr. Pharm. Des.*, 2005, **11**, 2577–2591.

3 A. Amoresano, A. Carpentieri, C. Giangrande, A. Palmese, G. Chiappetta, G. Marino and P. Pucci, *Clin. Chem. Lab. Med.*, 2009, **47**, 647–65.

4 Y. Yefremova, M. Al-Majdoub, K. F. M. Opuni, C. Koy, W. Cui, Y. Yan, M. L. Gross and M. O. Glocker, *J. Am. Soc. Mass Spectrom.*, 2015, **26**, 482–492.

5 B. Della Ventura, L. Schiavo, C. Altucci, R. Esposito and R. Velotta, *Biomed. Opt. Express*, 2011, **2**, 3223–3231.

6 R. Funari, B. Della Ventura, L. Schiavo, R. Esposito, C. Altucci and R. Velotta, *Anal. Chem.*, 2013, **85**, 6392–7.

7 R. Funari, B. Della Ventura, R. Carrieri, L. Morra, E. Lahoz, F. Gesuele, C. Altucci and R. Velotta, *Biosens. Bioelectron.*, 2015, **67**, 224–229.

8 E. V. Panfilova, B. N. Khlebtsov, A. M. Burov and N. G. Khlebtsov, *Colloid J.*, 2012, **74**, 99–109.

9 M. Banchelli, B. Tiribilli, M. de Angelis, R. Pini, G. Caminati and P. Matteini, *ACS Appl. Mater. Interfaces*, 2016, **8**, 2628–2634.

10 S. Dutta, N. Mandal and D. Bandyopadhyay, *Biosens. Bioelectron.*, 2016, **78**, 447–453.

11 E. Podstawka, Y. Ozaki and L. M. Proniewicz, *Appl. Spectrosc.*, 2004, **58**, 581–590.

12 B. Sjöberg, S. Foley, B. Cardey and M. Enescu, *Spectrochim. Acta Part A Mol. Biomol. Spectrosc.*, 2014, **128**, 300–311.

13 G. Zhu, X. Zhu, Q. Fan and X. Wan, *Spectrochim. Acta Part A Mol. Biomol. Spectrosc.*, 2011, **78**, 1187–1195.

14 S. Ngarize, H. Herman, A. Adams and N. Howell, *J. Agric. Food Chem.*, 2004, **52**, 6470–6477.

15 B. Fazio, C. D'Andrea, A. Foti, E. Messina, A. Irrera, M. G. Donato, V. Villari, N. Micali, O. M. Maragò and P. G. Gucciardi, *Sci. Rep.*, 2016, **6**, 26952.